

**Implications of the GALLEX Source Experiment
for the Solar Neutrino Problem**

Naoya Hata

Department of Physics, Ohio State University, Columbus, Ohio 43210

Wick Haxton

Institute for Nuclear Theory, NK-12, & Department of Physics, FM-15

University of Washington, Seattle, WA 98195

Abstract

We argue that, prior to the recent GALLEX ^{51}Cr source experiment, the excited state contributions to the ^{71}Ga capture cross section for ^{51}Cr and ^7Be neutrinos were poorly constrained, despite forward-angle (p,n) measurements. We describe the origin of the uncertainties and estimate their extent. We explore the implications of the source experiment for solar neutrino capture in light of these uncertainties. A reanalysis of the ^7Be and ^8B flux constraints and MSW solutions of the solar neutrino puzzle is presented.

Recently the GALLEX collaboration reported the first results of a ^{51}Cr neutrino source experiment [1]. The collaboration stressed the importance of this measurement as a test of experimental procedures, including the overall recovery efficiency of the product ^{71}Ge . This test is in addition to the run-by-run checks on the chemical extraction efficiency that have been performed by introducing Ge carrier. These have consistently indicated Ge yields of about 99% [2].

The significance of the source experiment is that it tests the recovery of ^{71}Ge under production conditions almost precisely mimicking those of solar neutrinos. For instance,

the recoil energies and atomic excitations accompanying solar neutrino absorption could conceivably drive a chemical reaction that would bind ^{71}Ge within the detector. This possibility is not entirely academic in view of the early GALLEX experience with cosmogenic ^{68}Ge ($\tau_{1/2} = 270.8$ d), which was not purged as expected from the detector when the experiment was begun [3]. Rather than continuing to decline exponentially, the ^{68}Ge level plateaued after repeated extractions at a level 20 times higher than the expected standard solar model (SSM) ^{71}Ge yield. While this difficulty was overcome by heating the tank, it illustrates that the chemistry of reactive species, when performed at levels below 100 atoms, can be subtle.

One motivation for the present study is to consider the role of excited states in ^{71}Ge in the capture of ^{51}Cr and ^7Be neutrinos. Electron capture on ^{51}Cr produces two line sources of neutrinos of energy 746 keV (90%) and 431 keV (10%). As illustrated in Fig. 1, the 431 keV neutrinos excite only the ground state of ^{71}Ge . The strength of this transition is fixed by the known lifetime of ^{71}Ge , 11.43 days, yielding

$$\text{BGT}(\text{gs}) = \frac{1}{2J_i + 1} |\langle J_f || O_{\text{GT}}^{J=1} || J_i \rangle|^2 = 0.087 \pm 0.001 \quad (1)$$

for the Gamow-Teller (GT) matrix element in the direction ^{71}Ga ($J_i^\pi = 3/2^-$) to ^{71}Ge ($J_f^\pi = 1/2^-$). The GT operator is

$$O_{\text{GT}}^{J=1} = \sum_{i=1}^A \vec{\sigma}(i) \tau_+(i). \quad (2)$$

However the dominant 746 keV branch can excite not only the ground state but also two other allowed transitions, to the $5/2^-$ (175 keV) and $3/2^-$ (500 keV) states in ^{71}Ge . These two excited states also contribute to the absorption of ^7Be solar neutrinos. The allowed transition strengths have not been measured directly, though arguments based on nuclear systematics and analyses of forward-angle (p,n) cross sections have led to a “standard” estimate of their contribution to the ^{51}Cr experiment of 5% [4]. The GALLEX collaboration adopted this estimate in deducing [1]

$$R = (1.04 \pm 0.12) \quad (1\sigma), \quad (3)$$

where R is the ratio of the measured ^{71}Ge atoms to expected in the source experiment.

Let us begin with a restatement of the source experiment result that is free of nuclear structure assumptions,

$$R_0 \equiv E \left[1 + 0.667 \frac{\text{BGT}(5/2^-)}{\text{BGT}(\text{gs})} + 0.218 \frac{\text{BGT}(3/2^-)}{\text{BGT}(\text{gs})} \right] = 1.09 \pm 0.13, \quad (4)$$

where $\text{BGT}(\text{gs})$, $\text{BGT}(5/2^-)$, and $\text{BGT}(3/2^-)$ are the Gamow-Teller strengths for the ground state and first two excited states in ^{71}Ge and E represents any deviation in the overall ^{71}Ge detection efficiency from that calculated and used by the experimentalists. The coefficients of the second and third terms within the brackets represent the phase space for exciting the 175 and 500 keV states by ^{51}Cr neutrinos, normalized to the ground state phase space. The experimental quantity R_0 is also normalized to the ground state contribution. Thus $R_0 = 1.05$ is the “standard” value corresponding to a 5% excited state contribution to the absorption of ^{51}Cr neutrinos.

If the excited states comprise only 5% of the ^{51}Cr neutrino capture rate, the transitions to these states must be roughly an order of magnitude weaker than to the ground state. Do we know this with certainty? We know of three arguments that address this issue:

1) Bahcall’s original estimate [5] of the strengths of the excited state matrix elements was made by examining known transitions in neighboring nuclei that connect states of the same spin and parity. In the case of the $3/2^-$ to $5/2^-$ transition, eight such decays were found, and from these Bahcall deduced $\text{BGT}(5/2^-) < 0.004$. Three or four of these decays, though not all, appear to be related to the Ga transition when viewed from the perspective of a single-particle model like that of Nilsson.

The neutron number of ^{71}Ga is 40; the analogous neutron numbers for the comparison transitions range from 33 to 38. Clearly one needs to assume that the nuclear structure is reasonably constant under addition of neutrons to use these data to extrapolate to the $N=40$ case of interest.

Both empirical and theoretical considerations indicate that this assumption is unwarranted. The empirical approach is to test this procedure in the case of the known $^{71}\text{Ga} \rightarrow ^{71}\text{Ge}(\text{gs})$ transition, $\text{BGT} = 0.087$. The most closely analogous neighboring decay is

$^{73}\text{Ga}(3/2^-) \rightarrow ^{73}\text{Ge}(1/2^-, 67 \text{ keV})$: In the Nilsson model this transition differs only by the addition of two spectator neutrons to the lowest deformed level based on the $1g_{9/2}$ spherical shell. Yet for this transition, $\text{BGT} = 0.0016$, or more than a factor of 50 weaker.

The theoretical considerations come from evidence [6,7] that the behavior of $N \sim 40$ Ge isotopes under changes in the neutron number is spectacularly nonlinear due to the interplay of coexisting spherical and deformed bands. Near $N=40$ it is possible to produce energetically favored, highly deformed neutron configurations in which a pair of neutrons occupies a Nilsson orbital based on the $1g_{9/2}$ spherical shell. This occupancy in turns polarizes and deforms the proton orbitals: the strong $1g_{9/2}(n)-1f_{5/2}(p)$ interaction (these shells have similar nodal structure) drives protons from the $2p_{3/2}$ shell into the $1f_{5/2}$ shell.

This explanation accounts for an apparent level crossing of the ground-state and first excited 0^+ bands in even- N Ge isotopes near $N=40$ (see Fig. 2 of Ref. [8]). Measurements show a corresponding sudden change in the shells occupied by the four valence protons: The ratio of the $2p_{3/2}$ and $1f_{5/2}$ spectroscopic factors plunges from 2.3 to 0.9 when two neutrons are added to ^{72}Ge (Fig. 3 of Ref. [8]). A large-basis shell model calculation has qualitatively reproduced this behavior, showing rapid changes in the proton occupancies between $N = 38$ and 42.

^{71}Ga (^{71}Ge) can be naively viewed as a proton (neutron) hole in a ^{72}Ge ($N=40$) core. As the core changes dramatically as the neutron number varies, β decay strengths might be expected to evolve sharply between $N=38$ and 42. Presumably this accounts for the disparity between the ^{71}Ga and ^{73}Ga BGT values noted above.

Similar arguments apply to the transition to the $3/2^-$ (500 keV) state. We conclude that systematics do not place quantitative constraints on the matrix elements of interest.

2) One could appeal to theory, but it is difficult to estimate weak BGT values reliably. Two credible attempts have been made, by Mathews et al. [9] and by Grotz, Klapdor, and Metzinger [10]. Their predictions are $\text{BGT}(5/2^-)/\text{BGT}(\text{gs}) = 0.23$ and 0.001 and $\text{BGT}(3/2^-)/\text{BGT}(\text{gs}) = 0.014$ and 0.86, respectively. Given the large discrep-

ancies, they provide little guidance. Neither calculation incorporates the physics that we argued in 1) drives the dramatic shape changes near $N=40$. For example, the polarizing $1f_{5/2}(p)-1g_{9/2}(n)$ interaction plays no role in the Mathews et al. calculation since neutrons are not allowed into the $1g_{9/2}$ shell.

3) We thus conclude that (p,n) reactions are the one hope for quantitatively constraining the unknown BGT values. At medium energies the proportionality between forward-angle cross sections and BGT strength has been well established [11] in the case of strong transitions ($BGT \gtrsim 0.4$). For this reason (p,n) mappings of the broad profile of BGT strength have been considered a valuable tool for estimating ${}^8\text{B}$ solar neutrino cross sections. However, it will become apparent below that the use of (p,n) reactions to constrain single transitions with small BGT strengths is a far more speculative endeavor.

Measurements for ${}^{71}\text{Ga}$ were made at 120 and 200 MeV by Krofcheck et al. [12], yielding

$$BGT_{(p,n)}(5/2^-) < 0.005 \quad \text{and} \quad BGT_{(p,n)}(3/2^-) = 0.011 \pm 0.002. \quad (5)$$

Perhaps because they conform to arguments based on systematics, these results appear to have been accepted rather uncritically.

But as these results are crucial to the interpretation of the calibration experiment, it is important to try to assess their likely reliability. Are (p,n) reactions a reliable probe of BGT values ~ 0.01 ? And if not, what is a reasonable error bar to assign to these determinations for very weak transitions?

We can try to answer these questions by examining (p,n) results for transitions of known strength. Ten transitions [13] for the $1p$ and $2s1d$ shell are shown in Table 1, including five mirror transitions where the nuclear structure is likely quite simple. In five cases the deduced (p,n) BGT values are quite large ($\gtrsim 1.0$), three are somewhat weaker ($\lesssim 0.5$), and two are very weak (~ 0.01 , comparable to the Krofcheck ${}^{71}\text{Ga}$ excited state BGTs). The correspondence between the (p,n) and β decay results for the five strong transitions is typically 10%, with one case showing a 30% discrepancy. The proportionality for the three weaker transitions is rather poor (typically off by a factor

of two). The discrepancies for the two very weak transitions are very large, as the (p,n) BGT values exceed the β decay values by factors of ~ 7 and ~ 100 .

The studies of Refs. [14] and [15] both identified an (L=2 S=1)J=1 term in the (p,n) operator as a likely source of these discrepancies. This operator arises in distorted wave Born treatments of (p,n) scattering and has been shown to affect weaker transitions in $^{37}\text{Cl}(p,n)^{37}\text{Ar}$ substantially (e.g., BGT $\lesssim 0.1$) [14]. Watson et al. [15] attributed the discrepancies in Table 1 to the effective tensor operator $O_{L=2}^{J=1}$

$$\langle J_f \| O_{(p,n)}^{J=1} \| J_i \rangle = \langle J_f \| O_{\text{GT}}^{J=1} \| J_i \rangle + \delta \langle J_f \| O_{L=2}^{J=1} \| J_i \rangle_{\text{SM}} \quad (6)$$

where

$$O_{L=2}^{J=1} = \sqrt{8\pi} \sum_{i=1}^A [Y_2(\Omega_i) \otimes \vec{\sigma}(i)]_{J=1} \tau_+(i). \quad (7)$$

In these studies values of the tensor operator coefficient $\delta = 0.073$ (0.064) were chosen for the 2s1d (1p) shell. The parameterization used in [15] would give $\delta = 0.097$ for ^{71}Ge . The notation $\langle \| \| \rangle_{\text{SM}}$ indicates that a shell model reduced matrix element is to be taken.

The operator $O_{(p,n)}^{J=1}$ defines an effective (p,n) BGT value, $\text{BGT}_{(p,n)}^{\text{eff}}$. The calculated values are given in Table 1. The shell model matrix elements of $O_{L=2}^{J=1}$ were evaluated using Cohen and Kurath [16] (1p shell) and Brown-Wildenthal [17] (2s1d shell) wave functions. We also take the sign of the interference between $O_{\text{GT}}^{J=1}$ and $O_{L=2}^{J=1}$ from the shell model. The magnitude of $\langle J_f \| O_{\text{GT}}^{J=1} \| J_i \rangle$ was taken from the β decay BGT values. The results match the measured $\text{BGT}_{(p,n)}$ rather well: Phenomenologically the differences between β decay and (p,n) BGT values do appear to be consistent with an additional L=2 tensor operator contributing to the latter. We determined δ by a least squares fit to the measured values, yielding $\delta = 0.069$ (0.096) for the 2s1d (1p) shells, results reasonably close to those recommended in Ref [15]. (Our treatment differs slightly from that of Ref. [15] because we express the difference in the (p,n) and β decay matrix elements as a shell model matrix element of an effective operator, rather than introducing effective operators for both (p,n) reactions and β decay. The resulting values for δ differ from those of Ref. [15] for this reason and because some of the β decay BGT values of Table 1 have been updated.)

This ansatz provides some insight into possible uncertainties in (p,n) BGT mappings. It is apparent, for very suppressed GT transitions, that (p,n) BGT values $\sim \delta^2 \sim 0.01$ can arise solely from the $L = 2$ contribution to Eq. (6). This accounts for the two most dramatic discrepancies in Table 1. (And as the (p,n) BGT values of Eq. (5) are $\lesssim 0.01$, it follows that these transitions could also be characterized by vanishing GT strengths.) The remaining significant discrepancies in Table 1 involve the analog transitions in ^{13}C , ^{15}N , and ^{39}K , which would be described naively as either $1p_{1/2} \rightarrow 1p_{1/2}$ or $1d_{3/2} \rightarrow 1d_{3/2}$ transitions. But for single-particle transitions with $\ell = j - 1/2$

$$\frac{\delta \langle J_f \| O_{L=2}^{J=1} \| J_i \rangle}{\langle J_f \| O_{\text{GT}}^{J=1} \| J_i \rangle} = 2\delta \left(\frac{\ell + 1}{2\ell - 1} \right). \quad (8)$$

Thus the $L=2$ and GT operators interfere constructively. This explains why the (p,n) BGT values of Table 1 are too large.

The case of ^{71}Ga is quite different, however. The $1/2^-$, $5/2^-$, $3/2^-$ level ordering in ^{71}Ge is consistent with a neutron shell of moderate positive deformation $\beta \sim 0.05 - 0.15$ in the Nilsson model. Thus the $5/2^-$ 175 keV state is likely associated with a neutron orbital that is almost entirely $1f_{5/2}$. We expect the valence protons to occupy the $2p_{3/2}$ shell, primarily. Thus the transition density [18] is likely dominated by

$$1f_{5/2}(n) \rightarrow 2p_{3/2}(p), \quad (9)$$

an amplitude that does not contribute to the GT operator but generates the strongest $L=2$ matrix element in the $1f2p$ shell. The competing GT amplitude would arise from presumably less important terms in the density matrix, e.g., $2p_{1/2} \rightarrow 2p_{3/2}$ and $1f_{5/2} \rightarrow 1f_{5/2}$. We have no experimental information on the relative sign of the $L=0$ and $L=2$ amplitudes.

The strength of this $L=2$ transition could quite plausibly approach the single-particle limit [19]. This provides the bound

$$|\delta \langle 5/2^- \| O_{L=2}^{J=1} \| 3/2^- \rangle_{\text{SM}}| \lesssim 6\delta \sqrt{\frac{3}{5}} = 0.45. \quad (10)$$

Using this constraint in Eqs. (5) and (6) then yields

$$0 \lesssim \text{BGT}(5/2^-) \lesssim 0.087. \quad (11)$$

That is, for destructive interference a BGT value on the order of $\text{BGT}(\text{gs})$ is not excluded by the (p,n) measurements.

The transition to the $3/2^-$ (500 keV) state is more complicated. In an effort to avoid exaggerating the BGT range, we take some guidance from the Nilsson model, which associates this state with a neutron hole in a $K=3/2$ orbital whose spherical parentage is $2p_{3/2}$, but which crosses and strongly mixes with a second $K=3/2$ orbital whose parentage is $1f_{5/2}$. We expect

$$\delta \langle 3/2^- \| O_{L=2}^{J=1} \| 3/2^- \rangle_{\text{SM}} \sim 6\delta \sqrt{\frac{3}{5}} \left[\Psi_{2p_{3/2}1f_{5/2}} + \frac{2}{9} \Psi_{2p_{3/2}2p_{3/2}} \right], \quad (12)$$

where $\Psi_{\alpha\beta}$ denotes components of the one-body transition density matrix [18]. But $\Psi_{2p_{3/2}2p_{3/2}}$ likely accounts for the largest contribution to the GT matrix element, too, to which it contributes with the same sign as above. Thus cancellation between the the $L=2$ and GT matrix elements likely requires cancellation between the density matrix elements in Eq. (12). We bound the $L=2$ matrix element by taking the single-particle limit under the Nilsson model constraint that $|\Psi_{2p_{3/2}1f_{5/2}}| \lesssim \frac{1}{\sqrt{2}}$,

$$|\delta \langle 3/2^- \| O_{L=2}^{J=1} \| 3/2^- \rangle_{\text{SM}}| \lesssim 6\delta \sqrt{\frac{3}{5}} \left(\frac{7}{9\sqrt{2}} \right) = 0.25. \quad (13)$$

Combining this with the (p,n) BGT value of 0.011 ± 0.002 yields

$$0 \lesssim \text{BGT}(3/2^-) \lesssim 0.057. \quad (14)$$

In their discussions of the implications of the source experiment for solar neutrino capture in ${}^{71}\text{Ga}$, the GALLEX collaboration fixed the ${}^{51}\text{Cr}$ excited state contributions at 5% and consider only the affects of shifting this strength between the $5/2^-$ and $3/2^-$ states. We now would like to make three observations based on the nuclear structure arguments of this paper.

i) Without the calibration experiment, no convincing argument exists for more restrictive bounds on $\text{BGT}(5/2^-)$ and $\text{BGT}(3/2^-)$ than those given by Eqs. (11) and (14), giving the region enclosed by the dashed lines in Fig. 2. These bounds allow the total excited state contribution to the ^{51}Cr capture rate to range between 0 and 80% of the ground state contribution, in contrast to the 5% employed in the GALLEX calibration discussions.

The other experimental checks [2] performed by the GALLEX collaboration make it likely that $E \sim 1.0$. We make this assumption now in order to explore the consequences of the nuclear physics uncertainties, independent of the question of efficiencies. It then follows that the pp capture rate is determined by the known value of $\text{BGT}(\text{gs})$. (The error associated with the 1% of captures to the first excited state is insignificant.) The ^8B capture rate depends on the broad profile of BGT strength up to the ^{71}Ge particle breakup threshold of 7.42 MeV. For states above 500 keV, we take the “best value” for this profile from Krofcheck et al., but associate a 1σ normalization uncertainty of 25%. [The Krofcheck profile was normalized by the isobaric analog state (IAS) transition. Uncertainties associated with this include the GT strength beneath the IAS peak, and the reliability of the calculated Fermi/GT strong distortion factor ratio. The 25% uncertainty results from empirical tests [11,20] of the IAS/Fermi proportionality [21]]. Finally, the ^7Be cross section has the large uncertainty associated with the freedom in $\text{BGT}(5/2^-)$ and $\text{BGT}(3/2^-)$, parameters for which we lack even best values.

Figures 3a, 3b, and 3c show the resulting constraints on $\phi(^7\text{Be})$ and $\phi(^8\text{B})$ that we have extracted from the GALLEX and SAGE [22] experiments, from GALLEX/SAGE in combination with Kamiokande II/III [23], and by considering all experiments (GALLEX, SAGE, Kamiokande II/III, and ^{37}Cl [24]) together. The χ^2 fits include the effects of pep and CNO neutrinos, and all fluxes are constrained by the condition that the solar luminosity is fixed [25]. The heavily shaded regions in these graphs indicate the allowed fluxes when the unknown BGT values are assigned their maximum values. These regions expand to include the lightly shaded portions when no excited state ^7Be capture is assumed. The

dashed line is the result using Krofcheck's BGT values. These graphs illustrate that the unknown nuclear physics induces a considerable uncertainty in the extracted bounds, represented by the lightly shaded regions, with large values of $\text{BGT}(5/2^-)$ and $\text{BGT}(3/2^-)$ leading to more stringent constraints on $\phi(^7\text{Be})$.

ii) If we now continue with the assumption that $E \sim 1.0$ but use the results on the source experiment, a constraint is imposed on the unknown BGT values,

$$\alpha \equiv 0.667 \frac{\text{BGT}(5/2^-)}{\text{BGT}(\text{gs})} + 0.218 \frac{\text{BGT}(3/2^-)}{\text{BGT}(\text{gs})} = 0.09 \pm 0.13 \quad (1\sigma), \quad (15)$$

where it is understood that this quantity is positive. This constraint significantly reduces the allowed region for the BGT values, as illustrated in Fig. 2. But more important, it almost completely removes the unconstrained nuclear physics uncertainties that affect the ^7Be capture rate. The capture rate can be reexpressed in terms of the constrained parameter α ,

$$\begin{aligned} \langle \sigma \phi(^7\text{Be}) \rangle &= (1.3 \text{ SNU}) P_{\text{MSW}}(384 \text{ keV}) + (34.4 \text{ SNU}) P_{\text{MSW}}(862 \text{ keV}) \\ &\times \left[1 + 1.09\alpha + 0.080 \left[-0.218 \frac{\text{BGT}(5/2^-)}{\text{BGT}(\text{gs})} + 0.667 \frac{\text{BGT}(3/2^-)}{\text{BGT}(\text{gs})} \right] \right], \quad (16) \end{aligned}$$

where P_{MSW} denotes a possible reduction in the 862 keV and 384 keV ^7Be line fluxes due to the Mikheyev-Smirnov-Wolfenstein (MSW) effect [26]. We have used the latest SSM fluxes of Bahcall and Pinsonneault (BP) [27] with He and metal diffusion in deriving Eq. (16) ($\phi(^7\text{Be}) = 5.15\text{E}9/\text{cm}^2\text{s}$). The last term (in brackets) on the right-hand side of Eq. (16) represents the degree of freedom in the $\text{BGT}(5/2^-) - \text{BGT}(3/2^-)$ plane that is orthogonal to α , and thus is unconstrained by the source experiment. The small coefficient of this term reflects the fact that the ^7Be and ^{51}Cr cross sections depend on nearly identical linear combinations of $\text{BGT}(5/2^-)$ and $\text{BGT}(3/2^-)$. Consequently, the residual, experimentally unconstrained nuclear physics uncertainties in the ^7Be cross section make at most a 3% contribution, given the bounds in Eqs. (11) and (14). Thus, in principle, a perfect ^{51}Cr source experiment could determine the ^7Be cross section to $\pm 1.5\%$. Future improvements in the source experiment will continue to be well motivated until a comparable statistical accuracy is achieved.

Presently, the uncertainty in the experimental constraint (Eq. (15)) is considerably larger than this $\pm 1.5\%$ “irreducible” error. However, as experiment has determined a “best value” and error for α , this constraint can now be included in the χ^2 fit. In Figs. 4 we present calculations analogous to those in Figs. 3, but with the source constraint included. Because the unconstrained uncertainties in the ${}^7\text{Be}$ cross section have been reduced to such a modest level, the boundaries of the allowed regions can now be represented accurately as lines.

The solar neutrino data, now with the gallium ${}^7\text{Be}$ cross section uncertainties clearly under control, are in serious conflict with suggested astrophysical explanations. Non-standard solar models generally reduce $\phi({}^8\text{B})$ more than $\phi({}^7\text{Be})$, in contradiction to the data (Fig. 4c). This difficulty persists when one considers only the SAGE/GALLEX and Kamiokande data (Fig. 4b), or any other pair of the SAGE/GALLEX, Kamiokande, and Homestake experiments (see, e.g., Ref [25]).

We can also now include the source experiment in fitting the results of the SAGE, GALLEX, Kamiokande II/III, and ${}^{37}\text{Cl}$ experiments in the presence of MSW oscillations. The MSW solutions provide an excellent description of the data, as shown in Fig. 5. We have assumed that the oscillation is into muon or tauon neutrinos, which will contribute to the Kamiokande II/III signal, though with a cross section about 1/7 that of electron neutrinos. The BP SSM with He and metal diffusion has again been used in the calculations. We have incorporated the theoretical uncertainties and their correlations, the Earth effect, the Kamiokande day-night data, and the improved definition of confidence level contours, following Ref. [28].

iii) We have assumed in our discussions that the relative efficiency E can be assumed to be unity. Even without this assumption, however, the ${}^7\text{Be}$ capture rate can be reexpressed in terms of the experimental quantity R_0 ,

$$\begin{aligned} \langle \sigma \phi({}^7\text{Be}) \rangle &= E(1.3 \text{ SNU}) P_{\text{MSW}}(384 \text{ keV}) + R_0(34.4 \text{ SNU}) P_{\text{MSW}}(862 \text{ keV}) \\ &\times \left[1 + \frac{0.043 \text{ BGT}(5/2^-) + 0.073 \text{ BGT}(3/2^-)}{\text{BGT}(\text{gs}) + 0.667 \text{ BGT}(5/2^-) + 0.218 \text{ BGT}(3/2^-)} \right]. \end{aligned} \quad (17)$$

The remaining nuclear structure uncertainties affecting the capture of 862 keV neutrinos

varies from 1.0 to 1.05, given the constraints (Eqs. (11) and (14)) on BGT(5/2⁻) and BGT(3/2⁻). Thus a measurement of R_0 with absolute precision would determine the overall ${}^{71}\text{Ga}$ detector ${}^7\text{Be}$ neutrino rate to $\pm 2.5\%$, independent of any assumptions about E .

If one adopts the extreme view that E is unconstrained apart from Eqs. (4), (11), and (14), the GALLEX result

$$\langle\sigma\phi\rangle_{{}^{71}\text{Ga}} = 79 \pm 10 \pm 6 \text{ SNU} \quad (1\sigma) \quad (18)$$

is not in serious conflict with the SSM: Maximal values for BGT(5/2⁻) and BGT(3/2⁻) allow E to be as low as 0.54, implying effective pp and ${}^8\text{B}$ neutrino counting rates of 38 and 9 SNU in the BP SSM. With a ${}^7\text{Be}$ neutrino rate of 38 SNU and pep and CNO cycle neutrino contributions of ~ 7 SNU, the observed counting rate would be ~ 90 SNU, within 1σ of the GALLEX best value. We are not advocating such a view, but instead pointing out the essential role the other checks on the chemical extraction and ${}^{71}\text{Ge}$ counting efficiencies still play in the gallium experiment. These checks are not superseded by the source experiment.

We thank E. Adelberger, S. Austin, N. Anantaraman, G. Bertsch, B. A. Brown, and especially P. Langacker for helpful discussions. This work was supported in part by the U.S. Department of Energy under grants #DOE-AC02-76-ERO-3071 and #DE-FG06-90ER40561 and by NASA under grant #NAGW2523.

Table 1: Comparison of experimental β -decay BGT values, experimental (p,n) BGT values, and $\text{BGT}_{(p,n)}^{\text{eff}}$ calculated from the effective operator of Eq. (6), using $\delta=0.069$ (0.096) for the 2s1d (1p) shell.

A_i	J_i	J_f (E_f (MeV))	Experiment		$\text{BGT}_{(p,n)}^{\text{eff}}{}^c$
			BGT a	$\text{BGT}_{(p,n)}^b$	
^{13}C	$1/2^-$	$1/2^-$ (0.0)	0.20	0.39	0.40
^{14}C	0^+	1^+ (3.95)	2.81	2.82	2.84
^{15}N	$1/2^-$	$1/2^-$ (0.0)	0.25	0.54	0.53
^{17}O	$5/2^+$	$5/2^+$ (0.0)	1.05	0.99	1.15
^{18}O	0^+	1^+ (0.0)	3.06	3.54	3.11
^{19}F	$1/2^+$	$1/2^+$ (0.0)	1.62	2.13	1.65
^{26}Mg	0^+	1^+ (1.06)	1.10	1.14	1.20
^{32}S	0^+	1^+ (0.0)	0.0021	0.014^d	0.016^e
^{39}K	$3/2^+$	$3/2^+$ (0.0)	0.27	0.39	0.39
^{39}K	$3/2^+$	$1/2^+$ (2.47)	0.00017	~ 0.017	0.014

a Deduced from the compilations of Ref. [29]

b From Ref. [15] unless otherwise noted.

c Matrix elements of $O_{L=2}^{J=1}$ and the sign of the interference between $O_{\text{GT}}^{J=1}$ and $O_{L=2}^{J=1}$ were evaluated with Cohen and Kurath (1p shell) and Brown-Wildenthal (2s1d shell) wave functions. The magnitudes of $\langle J_f || O_{\text{GT}}^{J=1} || J_i \rangle$ were taken from measured β decay ft values.

d From Ref. [20].

e For this transition the calculated β decay BGT is so small ($5 \cdot 10^{-5}$) that theory cannot reliably determine the sign of the interference between $O_{\text{GT}}^{J=1}$ and $O_{L=2}^{J=1}$. We have assumed constructed interference.

References

- [1] The GALLEX Collaboration, P. Anselmann et al., *Phys. Lett. B* 342 (1995) 440.
- [2] The GALLEX Collaboration, P. Anselmann et al., *Phys. Lett. B* 285 (1992) 376, 314 (1993) 445, and 327 (1994) 377.
- [3] See, for example, T. Kirsten, *Nucl. Phys. B (Proc. Suppl.)* 28 A (1992).
- [4] J. N. Bahcall and R. K. Ulrich, *Rev. Mod. Phys.* 60 (1988) 297.
- [5] J. N. Bahcall, *Rev. Mod. Phys.* 50 (1978) 881.
- [6] M. Vergnes, talk presented at the Int. Conf. on the Structure of Medium-Heavy Nuclei, Rhodes, Greece (1979); M. Vergnes et al., *Phys. Lett. B* 72 (1978) 447.
- [7] D. Ardouin et al., *Phys. Rev C* 18 (1978) 1201; G. Rotbard et al., *Phys. Rev. C* 18 (1978) 86; S. Mordechai, H. T. Fortune, R. Middleton, and G. Stephans, *Phys. Rev. C* 18 (1978) 2498.
- [8] W. C. Haxton, in *Nuclear Beta Decay and the Neutrino*, ed. T. Kotani, H. Ejiri, and E. Takasugi (World Scientific, Singapore, 1986), p. 225.
- [9] G. J. Mathews, S. D. Bloom, G. M. Fuller, and J. N. Bahcall, *Phys. Rev. C* 32 (1985) 796.
- [10] K. Grotz, H. V. Klapdor, and J. Metzinger, *Astron. and Astrophys.* 154 (1986) L1.
- [11] See, e.g., T. N. Taddeucci et al., *Nucl. Phys. A* 469 (1987) 125.
- [12] D. Krofcheck et al., *Phys. Rev. Lett.* 55 (1985) 1051; D. Krofcheck, Ph.D. thesis, Ohio State University (1987).
- [13] Taken from the compilation of Ref. [15].
- [14] S. M. Austin, N. Anantaraman, and W. G. Love, *Phys. Rev. Lett.* 73 (1994) 30.

- [15] J. W. Watson et al., Phys. Rev. Lett. 55 (1985) 1369.
- [16] S. Cohen and D. Kurath, Nucl. Phys. 73 (1965) 1.
- [17] B. H. Wildenthal, Prog. Part. Nucl. Phys. 11 (1984) 5.
- [18] The many-body matrix element of any one-body operator is given exactly by the one-body density matrix $\Psi_{\alpha\beta}$,

$$\langle J_f \| O^{J=1} \| J_i \rangle = \sum_{\alpha\beta} \Psi_{\alpha\beta}^{J=1} \langle \alpha \| O^{J=1} \| \beta \rangle,$$

where the sum extends over a complete set of single-particle quantum numbers α and β . The finite Hilbert spaces used in shell model calculations approximate this expression by truncating the sums. The usual model space choice for A=71 is $2p_{3/2}-1f_{5/2}-2p_{1/2}-1g_{9/2}$. Regardless of the complexity of the many-body calculation within this space, the matrix element of $O_{(p,n)}^{J=1}$ can be written

$$\begin{aligned} & -\Psi_{55}\sqrt{\frac{30}{7}}(1 + \frac{8}{5}\delta) + 2\Psi_{33}\sqrt{\frac{5}{3}}(1 + \frac{2}{5}\delta) - \frac{4}{3}\sqrt{3}\Psi_{31}^-(1 - \frac{\delta}{2}) \\ & -\sqrt{\frac{2}{3}}\Psi_{11}(1 + 4\delta) + 6\delta\sqrt{\frac{3}{5}}\Psi_{35}^- + \sqrt{\frac{110}{9}}\Psi_{99}(1 + \frac{8}{11}\delta), \end{aligned}$$

where $\Psi_{55} = \Psi_{1f_{5/2}1f_{5/2}}$, etc., and $\Psi_{31}^- = \Psi_{31} - \Psi_{13}$, etc. However, different model calculations may differ substantially in their predictions for the Ψ s.

- [19] In the limit where the initial ^{71}Ga and final ^{71}Ge states are simple $2p_{3/2}$ proton and $1f_{5/2}$ neutron holes in a closed ^{72}Ge core, respectively, the only nonzero transition density matrix element is $\Psi_{35} = 1$. This is the maximum strength for states that can be written as simple Slater determinants. If one introduces correlations, it is possible for Ψ_{35}^- to exceed this single-particle limit. But, as the magnitude of Ψ_{53} is expected to be small, we take the single-particle bound as an effective upper limit for Ψ_{35}^- .

- [20] B. Anderson, in Proc. GT and Neutrino Cross Section Workshop, ed. K. Lande (Univ. of Pennsylvania, unpublished), chapt. 13.
- [21] One might be tempted to assume that the ^{71}Ga normalization is more accurate, since the (p,n) value for BGT(gs) agrees beautifully with the β decay result. But, as we have seen that the β decay/(p,n) proportionality is unreliable for weak transitions, this agreement is not a strong validation of the IAS normalization.
- [22] J. N. Abdurashitov et al., Phys. Lett. B 328 (1994) 234; J. Nico, talk presented at the Int. Conf. High Energy Physics, Glasgow, July, 1994.
- [23] The Kamiokande Collaboration, K. S. Hirata et al., Phys. Rev. D 38 (1988) 448 and 44 (1991) 2241; Phys. Rev. Lett. 65 (1990) 1297, 65 (1990) 1301, and 66 (1991) 9; K. Nakamura, to be published in Proc. Int. Conf. on Non-Accelerator Particle Physics (India) 1994.
- [24] B. T. Cleveland et al., Nucl. Phys. B (Proc. Suppl.) 38 (1995) 47; R. Davis, Jr., in Frontiers of Neutrino Astrophysics, ed. Y. Suzuki and K. Nakamura (University Academy Press, Tokyo, 1993) p. 47.
- [25] These procedures follow N. Hata, S. Bludman, and P. Langacker, Phys. Rev. D. 49 (1994) 3622 and N. Hata and P. Langacker, Univ. of Pennsylvania Report No. UPR-0625T (1994), to be published in Phys. Rev. D.
- [26] S. P. Mikheyev and A. Yu. Smirnov, Sov. J. Nucl. Phys. 42 (1985) 913 and Nuovo Cimento 9C (1986) 17; L. Wolfenstein, Phys. Rev. D 17 (1978) 2369 and 20 (1979) 2634.
- [27] J. N. Bahcall and M. H. Pinsonneault, submitted to Rev. Mod. Phys. and Rev. Mod. Phys. 64 (1992) 885.
- [28] S. Bludman, N. Hata, D. Kennedy, and P. Langacker, Phys. Rev. D 47 (1993) 2220; N. Hata and P. Langacker, Phys. Rev. D 48 (1993) 2937 and D 50 (1994) 632.

- [29] B. A. Brown and B. H. Wildenthal, *Atomic Data and Nuclear Data Tables* 33 (1985) 347; W. T. Chou, E. K. Warburton, and B. A. Brown, *Phys. Rev. C* 47 (1993) 163.

Figure Captions

- [1] Level scheme for ^{71}Ge showing the excited states that contribute to absorption of pp, ^7Be , ^{51}Cr , and ^8B neutrinos.
- [2] Constraints imposed on $\text{BGT}(5/2^-)$ and $\text{BGT}(3/2^-)$ by Krofcheck et al. [12] (small shaded region), by the present reanalysis of the (p,n) results (area enclosed by the dashed lines), and by the ^{51}Cr source experiment (diagonal lines).
- [3] The 90% C.L. limits on $\phi(^7\text{Be})$ and $\phi(^8\text{B})$ imposed by the SAGE and GALLEX experiments (a), by SAGE, GALLEX, and Kamiokande (b), and by SAGE, GALLEX, Kamiokande, and ^{37}Cl (c). $\phi(^7\text{Be})$ and $\phi(^8\text{B})$ are in the SSM units of $4.89\text{E}9/\text{cm}^2 \text{ s}$ and $5.69\text{E}6/\text{cm}^2 \text{ s}$, respectively. The allowed regions are shaded. The heavily shaded region corresponds to the choice of maximum values for $\text{BGT}(5/2^-)$ and $\text{BGT}(3/2^-)$ (so that excited state contributions to ^7Be neutrino capture are $\sim 90\%$ of the ground state contribution), while the entire shaded region is allowed if no ^7Be neutrino excited state capture occurs. Thus the difference (the lightly shaded region) represents the effects of nuclear structure uncertainties on the extracted flux bounds prior to the source experiment. The dotted line gives the result for Krofcheck et al. [12] BGT values. Note that Fig. 3c also includes 99% C.L. limits (left unshaded for clarity).
- [4] As in Figs. 3, but with the source experiment constraint on $\text{BGT}(5/2^-)$ and $\text{BGT}(3/2^-)$ now included in the χ^2 fit. The residual unconstrained nuclear structure uncertainties are so small that they are not shown (see text). Also shown in (b) and (c) are various standard and nonstandard solar model predictions (see Ref. [25] and references therein).
- [5] The MSW oscillation parameters allowed by the combined results of the SAGE, GALLEX, Kamiokande, and ^{37}Cl experiments, incorporating the uncertainties in $\text{BGT}(5/2^-)$ and $\text{BGT}(3/2^-)$ determined by the ^{51}Cr source experiment. We have employed the fluxes from the BP SSM with He and metal diffusion [27].

This figure "fig1-1.png" is available in "png" format from:

<http://arxiv.org/ps/nucl-th/9503017v1>

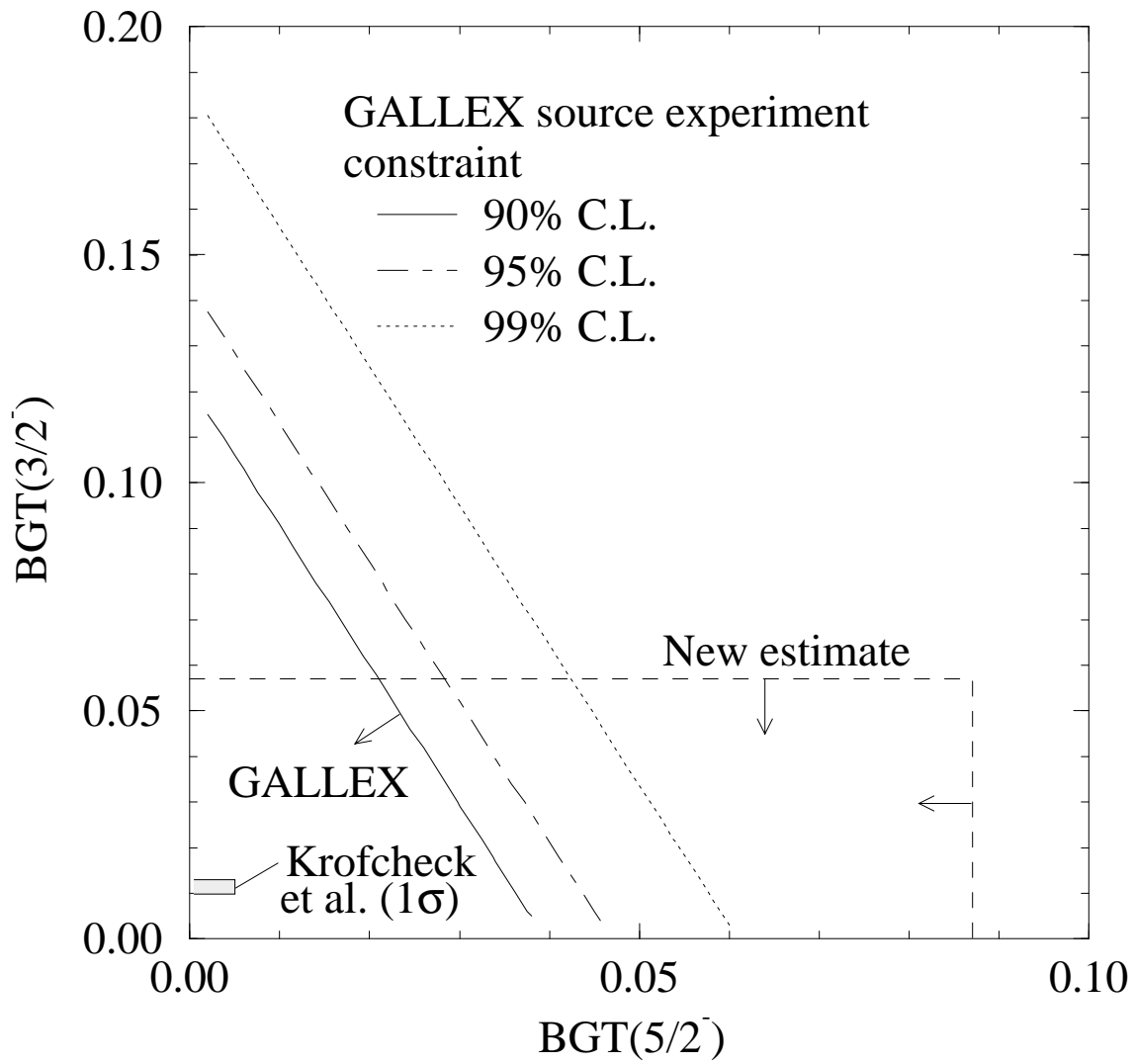


Figure 2

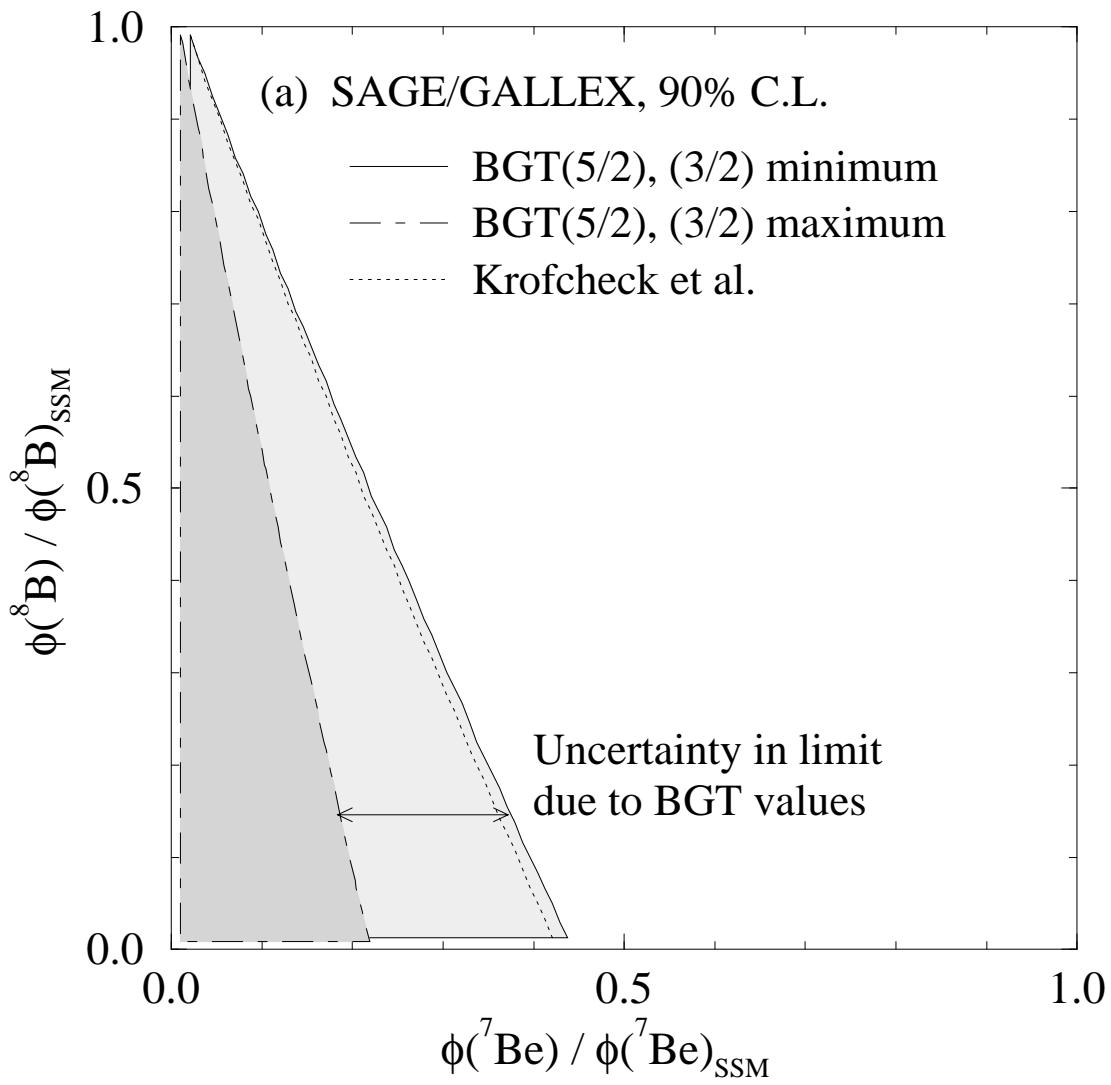


Figure 3(a)

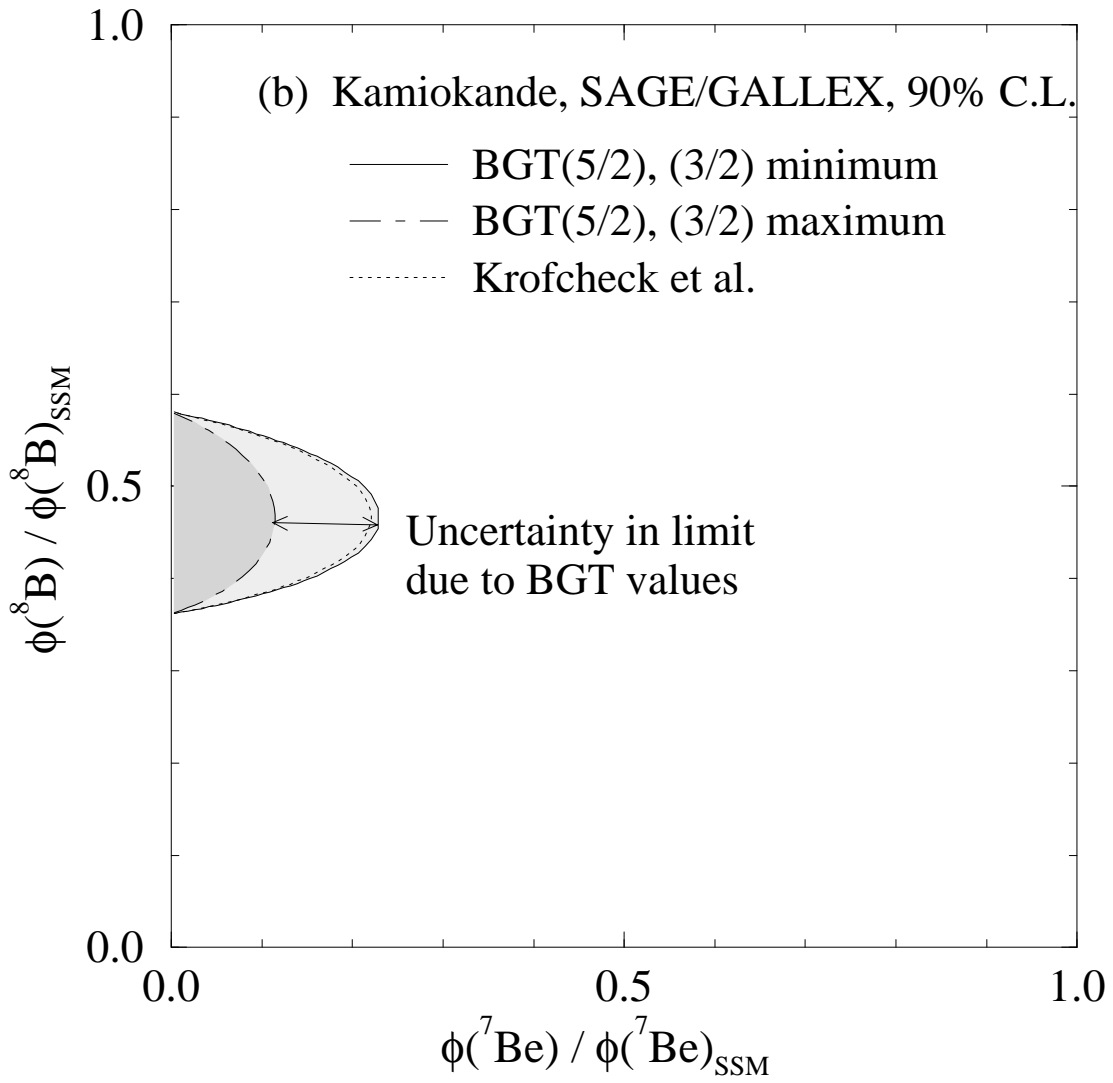


Figure 3(b)

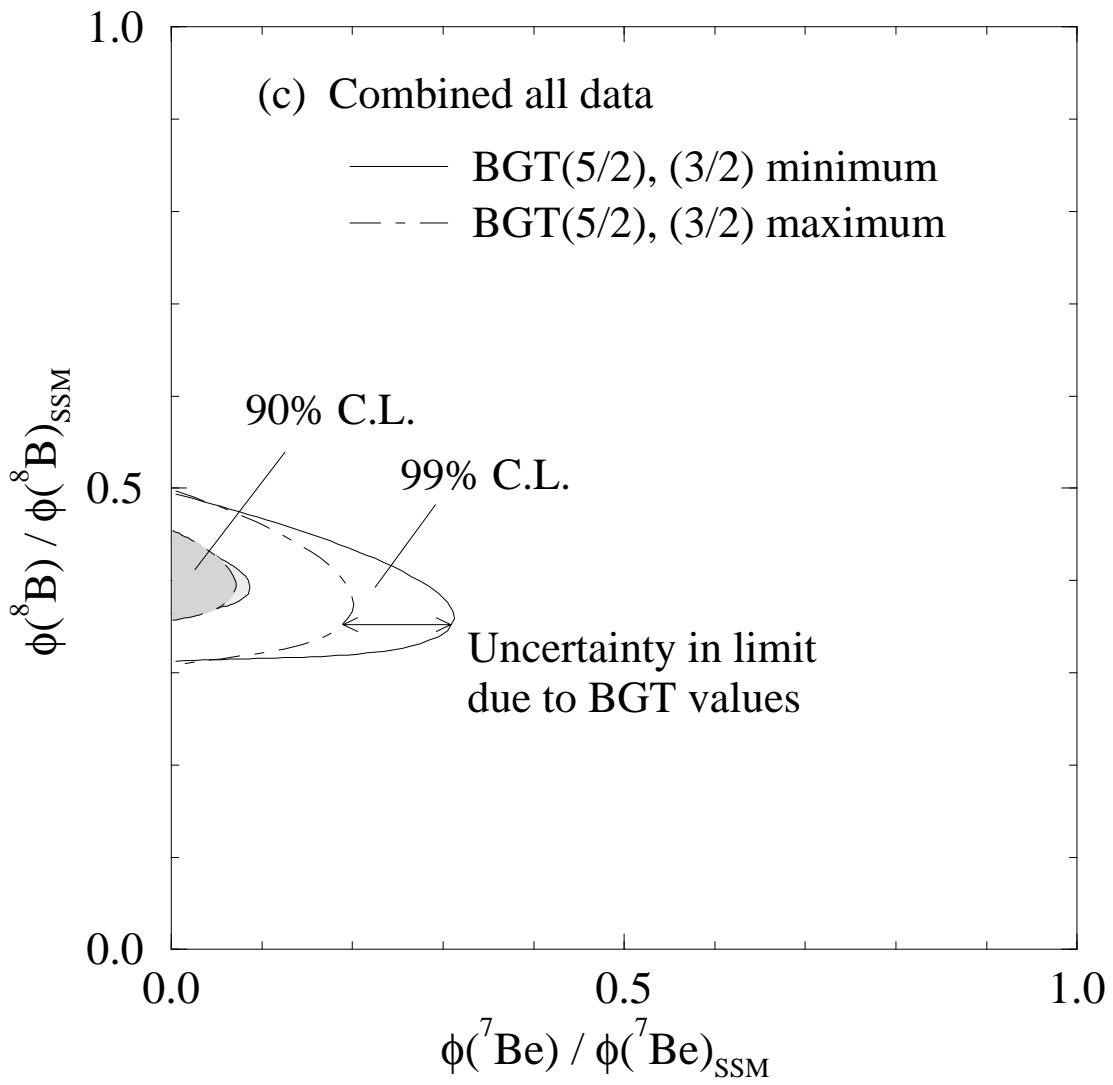


Figure 3(c)

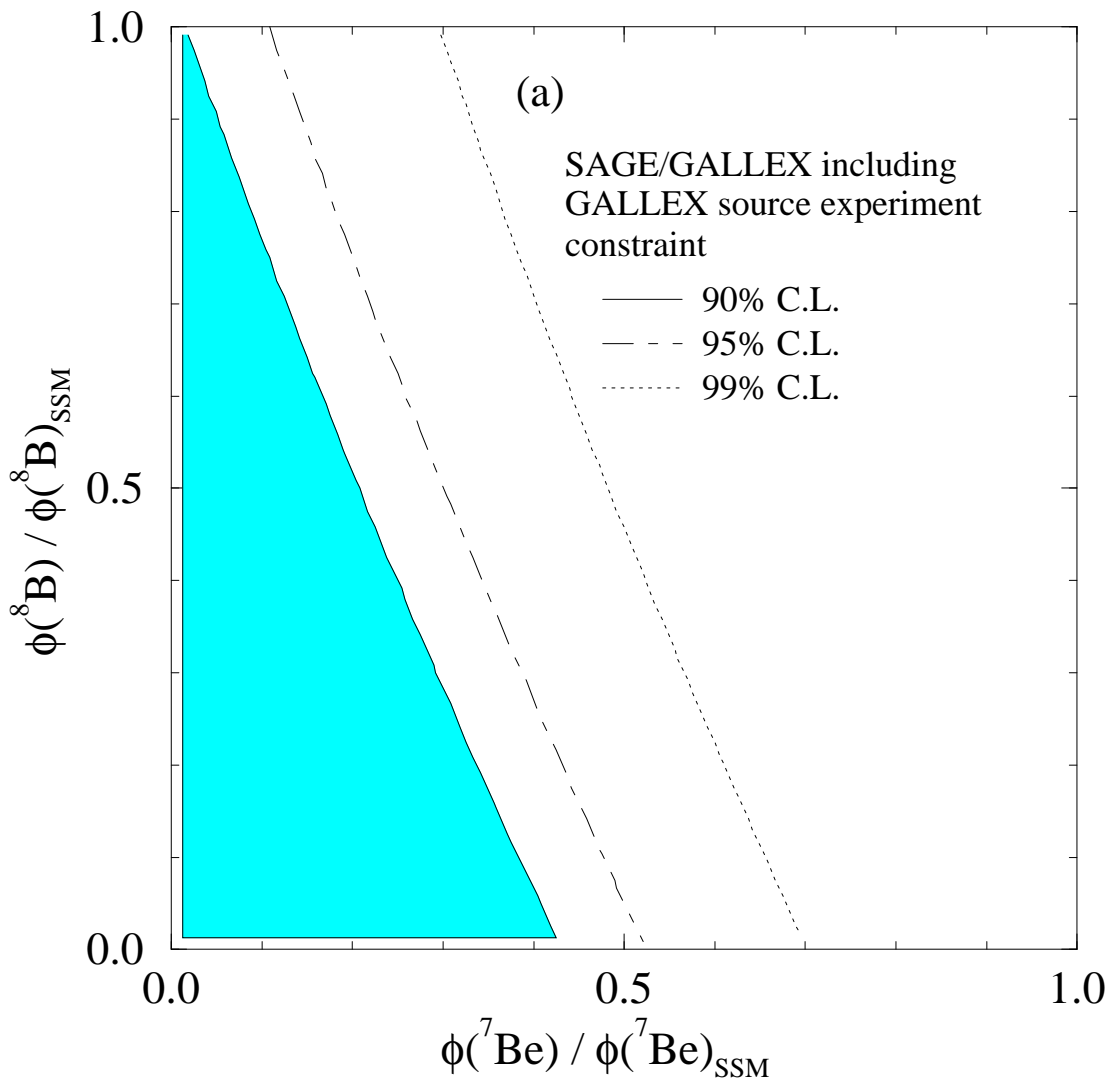


Figure 4(a)

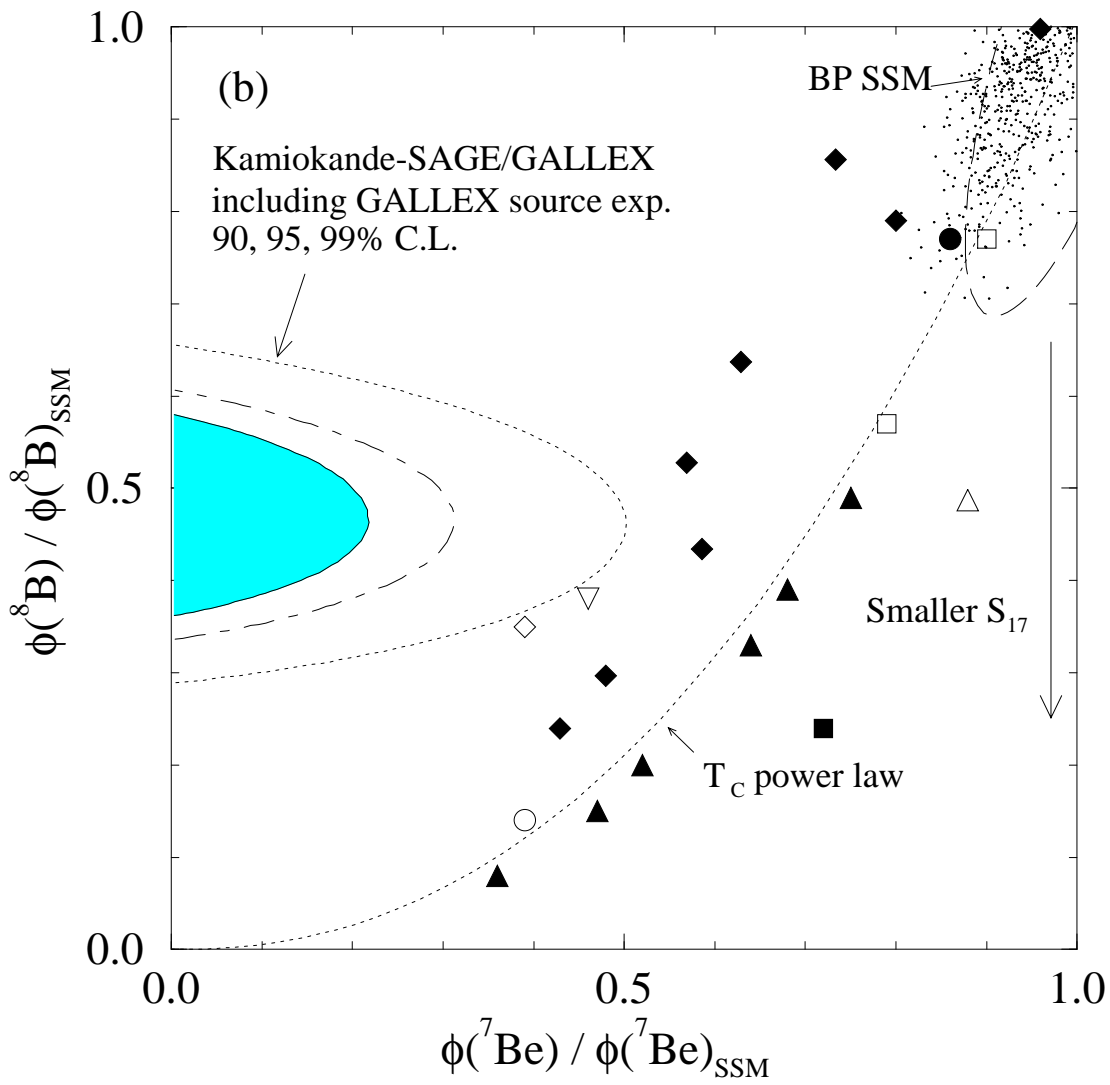


Figure 4(b)

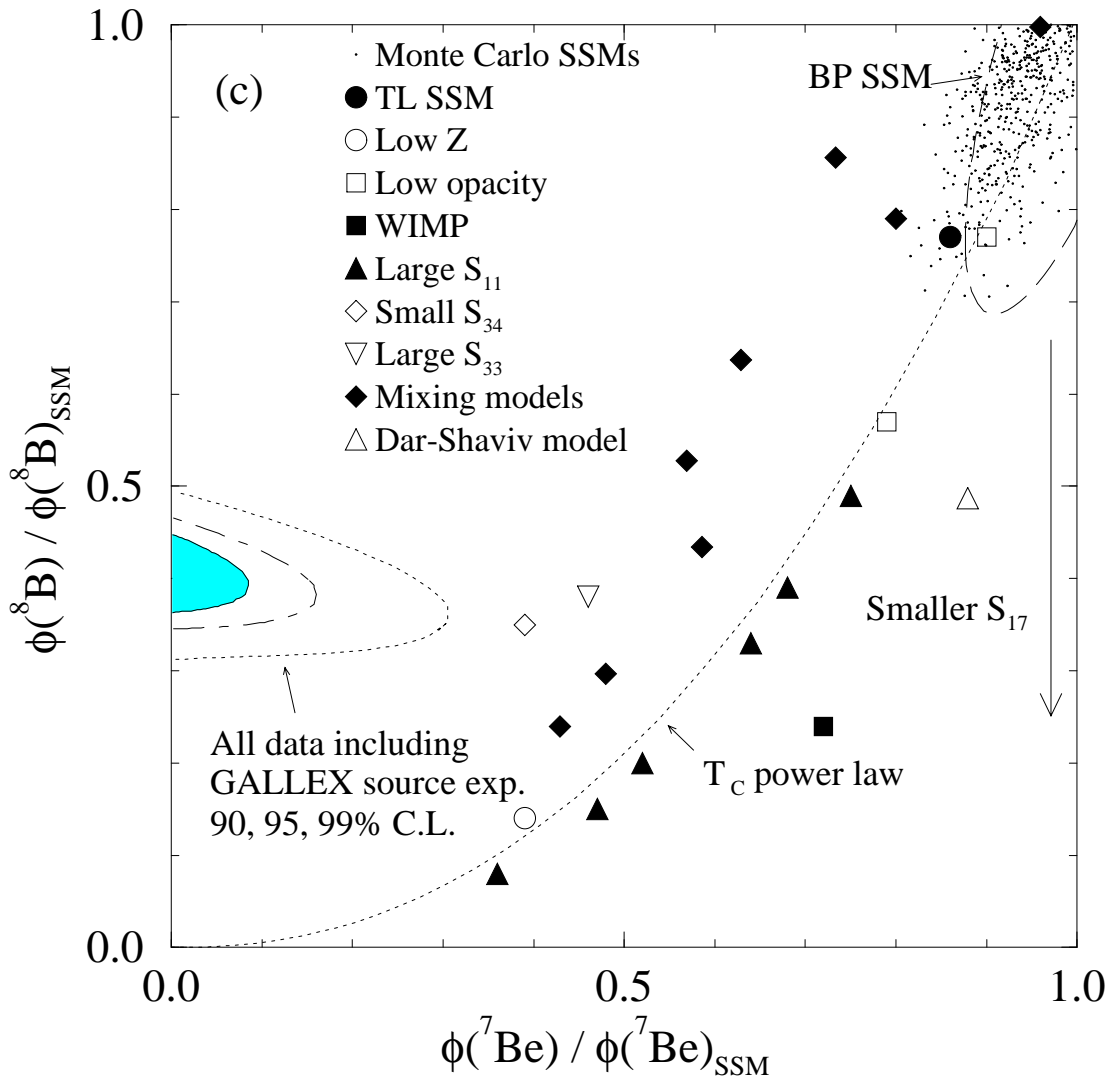


Figure 4(c)

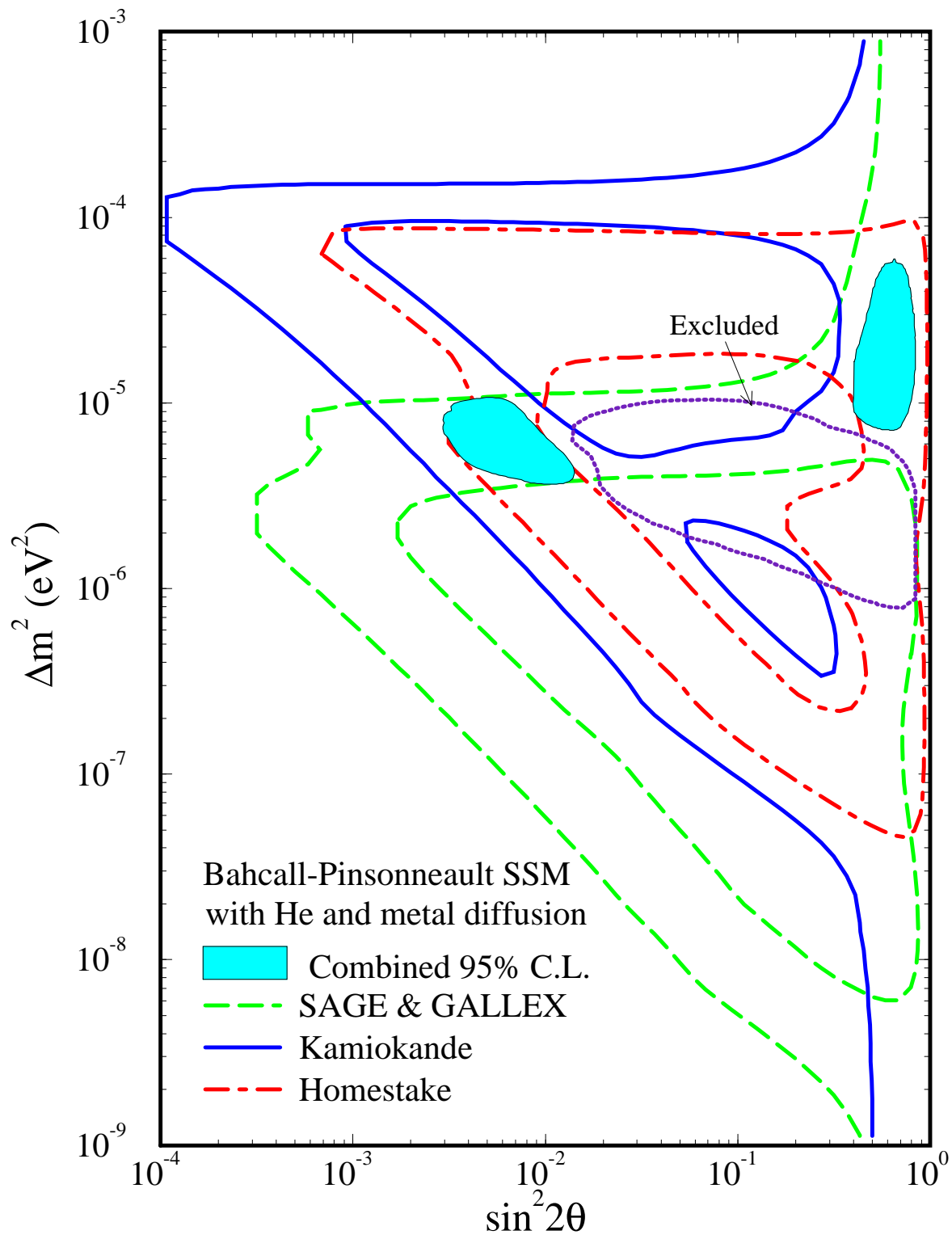


Figure 5